Topographic guidance of endothelial cells on silicone surfaces with micro- to nanogrooves: Orientation of actin filaments and focal adhesions

Pimpon Uttayarat,[1] George K. Toworfe,[1] Franziska Dietrich,[2] Peter I. Lelkes,[2] Russell J. Composto[1]
[1]*Department of Materials Science and Engineering, University of Pennsylvania, 3451 Walnut Street, Philadelphia, Pennsylvania 19104*
[2]*School of Biomedical Engineering, Science, and Health Systems, Drexel University, 3141 Chestnut Street, Philadelphia, Pennsylvania 19104*

Received 4 March 2005; revised 18 April 2005; accepted 19 May 2005
Published online 18 August 2005 in Wiley InterScience (www.interscience.wiley.com). DOI: 10.1002/jbm.a.30478

Abstract: To mimic the uniformly elongated endothelium in natural linear vessels, bovine aortic endothelial cells (BAECs) are cultured on micro- to nanogrooved, model poly(dimethylsiloxane) (PDMS) substrates preadsorbed with about 300 ng/cm^2 of fibronectin. BAEC alignment, elongation, and projected area were investigated for channel depths of 200 nm, 500 nm, 1 μm, and 5 μm, as well as smooth surfaces. Except for the 5 μm case, the ridge and channel widths were held nearly constant about 3.5 μm. With increasing channel depth, the percentage of aligned BAECs increased by factors of 2, 2, 1.8, and 1.7 for 1, 4, 24, and 48 h. Maximum alignment, about 90%, was observed for 1 μm deep channels at 1 h. The alignment of BAECs on grooved PDMS was maintained at least until cells reached near confluence. F-actin and vinculin at focal adhesions also aligned with channel direction. Analysis of confocal microscopy images showed that focal adhesions localized at corners and along the sidewalls of 1-μm deep channels. In contrast, focal adhesions could not form on the bottom of the 5-μm deep channels. Cell proliferation was similar on grooved and smooth substrates. In summary, PDMS substrates engraved with micro- and nanochannels provide a powerful method for investigating the interplay between topography and cell/cytoskeletal alignment. © 2005 Wiley Periodicals, Inc. J Biomed Mater Res 75A: 668–680, 2005

Key words: cell alignment; substrate topography; endothelial cells; focal adhesions; poly(dimethylsiloxane)

INTRODUCTION

A major problem with synthetic vascular grafts, particularly for diameters less than 4 mm,[1] is thrombus and neointima formation. One approach to prevent thrombosis and to improve the biocompatibility of synthetic grafts is to create a functional, quiescent monolayer of endothelial cells on the graft surface.[1] For the case of a polymeric template, successful adhesion of endothelial cells to a typically inert, unmodified polymer depends on the chemical constitution of the surface. Surface modifications, such as the adsorption of extracellular matrix (ECM) proteins[2–4] and the covalent attachment of specific RGD peptide sequences,[1,5–7] have been found to promote endothelial cell adhesion onto a variety of synthetic materials. Relative to studies involving surface chemistry, systematic studies of surface topography have only recently received significant attention. To date, topographic features have been shown to incite changes in the morphology and orientation of adherent endothelial cells.[4,8] By combining surface chemistry and surface topography, endothelial cell adhesion and orientation on polymeric synthetic grafts can be controlled to mimic the shear-resistant aligned, elongated endothelium found in linear vessels.[9]

Weiss[10–12] introduced the concept of contact guidance to describe cell orientation and cell locomotion in response to topographic underlying substrata. Subsequently, contact guidance of diverse cell types such as neurons,[10–12] fibroblasts,[13–16] endothelial,[2,4,8] epithelial,[15,17] BHK,[18,19]MDCK,[19] macrophages,[20,21] and neutrophils[20,22] has been observed for a variety of topographic textures, including grooves,[4,13,15,17–22] pillars,[2] waves,[8] and fibers.[10–12,14] For groove patterns consisting of ridges and channels, strong alignment in the channel direction was achieved by either varying the

Correspondence to: R. Composto; e-mail: composto@seas.upenn.edu
Contract grant sponsor: grants-in-aid from the Nanotechnology Institute of Southeastern Pennsylvania (to R.J.C. and P.I.L.)

ridge width[16,18] or channel depth.[18,19] In either case, most cells were distinctly aligned for ridge (4 μm[16]) and groove (6 μm[19]) widths narrower than the cell diameter (10–20 μm[23]) in suspension. In accordance with changes in cell orientation, fluorescently labeled F-actin[4,8,13,18,24] and actin-associated proteins, such as vinculin at focal adhesions,[4,8,24] were observed to align in the direction of the channels. Besides inducing changes in cell orientation, contact guidance has also been reported to stimulate growth,[23] protein synthesis,[25] proteinase secretion,[26] and phagocytosis activities[21] in various cell types.

Although it is widely recognized that cells and their intracellular proteins orient parallel to grooved surfaces, the mechanism by which cells "sense" the topographical variation and undergo morphological changes is not well understood. In this study, we fabricated elastomeric PDMS as a model substrate, displaying channels and ridges with a pitch of 8 μm. The channel depth was systematically varied from 200 nm to 5 μm to investigate whether an optimum depth or minimal response could be observed. By preadsorbing PDMS substrates with the uniform coverage of fibronectin (Fn), differences in cell alignment and intracellular protein alignment can be attributed to the variation in the substrate feature size. The alignment, elongation and area of BAECs were quantified after 1, 4, 24, and 48 h incubation. In all cases, the percentage of aligned cells increased as channel depth increased from 200 nm to 1 μm. A slight decrease in alignment was observed at 1, 4, and 24 h on the 5-μm deep channels. This alignment of cells was maintained at near confluence, indicating that the uniformly elongated endothelium, as naturally found in linear vessels,[9] can be achieved on the chemically and physically modified PDMS substrates. Whereas maximum cell alignment was achieved after 1 h, F-actin and focal adhesions continued to align and increase their concentrations, reaching a maximum after about 24 h. Providing new insight into the mechanism of cell orientation, focal adhesions were observed to preferentially localize along the edge of ridges and channels as well as along the sidewalls of the channel.

MATERIALS AND METHODS

Materials

Silicon (Si) wafers ⟨100⟩ were purchased from Silicon Quest International (Santa Clara, CA). Negative resist, RD6 developer, and RR2 remover were purchased from Futurrex (Franklin, NJ). Sylgard 184 to prepare crosslinked PDMS was purchased from Robert McKeown Company, Inc (Branchburg, NJ). Fn, gelatin, thiorhodamine isothiocyanate (TRITC)-labeled phalloidin, and sodium cacodylate were purchased from Sigma (St. Louis, MO). Bovine serum albumin (BSA), formaldehyde, and gluteraldehyde were purchased from Fisher (Newark, DE). Oregon Green 488 fluorochrome was purchased from Molecular Probes (Eugene, OR). Mouse monoclonal antivinculin IgG_1 and fluorescein isothiocyanate (FITC)-conjugated goat antimouse IgG were purchased from Chemicon (Temecula, CA). Vectashield with DAPI was purchased from Vector Laboratories (Burlingame, CA).

TABLE I
Reactive Ion Etch Parameters and Channel Depth in Si Molds

Channel Depth	Gas Flow Rate (sccm)			Pressure (mTorr)	Etch Time (min)
	CF_4	SF_6	O_2		
200 nm	20	5	5	15	2.30
500 nm	20	5	5	15	3.30
1 μm	20	7	5	15	14.00
5 μm	20	7	5	20	20.00

Microfabrication of silicon mold

To create grooved PDMS substrates with vertical sidewalls, a silicon mold was prepared with controlled channel and ridge widths, and most importantly, a systematic variation in channel depth. All Si molds were fabricated using photolithography and reactive ion etching (RIE) techniques at the Microfabrication Facility, University of Pennsylvania. Si wafers were first cleaned in a deionized water–sulfuric acid mixture (1:2) at 120°C for 10 min, followed by rinsing in deionized water and drying with nitrogen gas. The negative resist was spun-coated onto Si at 3000 rpm for 40 s to generate a uniform 1-μm thick film. After UV exposure during pattern transfer, the resist was developed and then dried under nitrogen. These resist-patterned wafers were then immediately coated by e-beam evaporation (house-assembled; Thermionics Vacuum Products, Port Townsend, WA) with Nichrome IV (80% Ni and 20% Cr) at 1217°C and 10^{-6} Torr to generate a 100 nm-thick photomask. After removing Nichrome IV-coated resist regions with RR2 solution, only remaining stripes of Nichrome IV served as photomask for subsequent RIE.

The patterned Si wafers with Nichrome IV photomask were dry etched with RIE (PlasmaLab μP, Bid Service, Freehold, NJ) to create channels with depths of 200 nm, 500 nm, 1 μm, and 5 μm. The RF power and the DC bias were set at 150 W and 380 V, respectively. The flow rates of CF_4, SF_6, and O_2, the pressure, and the etch time used to achieve channel depths from 200 nm to 5 μm are given in Table I. After RIE, the photomask was removed in a solution containing 155 g ceric ammonium nitrate, 60 mL nitric acid, and 985 mL deionized water. The four Si molds were then rinsed in deionized water and dried under nitrogen.

Smooth and grooved PDMS substrates

Smooth and grooved PDMS substrates with a thickness of 1 mm were cast using Sylgard 184. After thoroughly mixing

a 10:1 ratio of base resin to curing agent, the mixture was poured either into Si molds or a polystyrene Petri dish to create grooved or smooth substrates, respectively. After curing at room temperature for 48 h, the PDMS substrates were cut into circles using a hole puncher (2 cm diameter) and then annealed at 65°C for 3 h to ensure the complete crosslinking. The resulting PDMS replicas exhibited nearly equal ridge and channel widths, about 4 μm, for channel depths of 200 nm, 500 nm, and 1 μm. For the 5-μm channel depth, however, the channel width was narrower, about 2 μm, with a ridge width of 5 μm. These dimensions were used to determine if a slight variation in the lateral spacing of ridges and channels would impact cell orientation.

The grooved PDMS substrates were examined by atomic force microscopy (AFM, Digital Instruments Dimension 3000) and scanning electron microscopy (SEM, JEOL 6400). For the smooth PDMS substrates, surface roughness and water contact angle were obtained from AFM and the sessile drop method,[27] respectively. All samples were ultrasonically cleaned twice in ethanol for 30 min to leach residual monomer. The PDMS substrates were then sterilized under UV and dried overnight in a cell culture hood.

Fibronectin adsorption and characterization

Both smooth and grooved PDMS substrates were immersed in a 10 μg/mL Fn in phosphate buffered saline (PBS) solution at 37°C. This concentration is known to produce a monolayer coverage on hydrophobic surfaces.[28] Adsorption times were 1 h for smooth, 200-nm and 500-nm PDMS, while it was increased to 15 h for 1-μm and 5-μm PDMS to ensure that channels exhibited monolayer coverage of Fn. The Fn coverage was quantified following the procedure of Toworfe et al.[27] Briefly, prelabeled Fn (*Fn) was adsorbed onto PDMS surfaces according to the previous procedure for analysis in a fluorescence microplate reader (Spectrafluor Plus, TECAN) at 485 nm excitation and 535 nm emission. The fluorescence intensity was used to determine the *Fn surface densities (ng/cm^2) on smooth and grooved PDMS.

For cell culture, nonspecific attachment to Fn-coated substrates was blocked by immersion in a 1% BSA solution[28] for 30 min at 37°C. After washing twice with PBS, the PDMS samples were ready for cell culture.

Cell culture

BAECs were isolated as described[29] and cultured in gelatin-coated T75 flasks using Dulbecco's Modification of Eagle's Medium (DMEM) supplemented with 10% fetal bovine serum (FBS), 1 mg/mL glucose, 0.3 mg/mL L-glutamine, 10 μg/mL streptomycin, 10 U/mL penicillin, and 25 ng/mL amphotericin at 37°C in 95% air/5% CO_2. Cells were subcultured every 2 days. Cell at passages 9–16 were used in the experiments. In preliminary experiments we established that differences in passage numbers did not affect the outcome of our study (e.g., alignment, proliferation).

BAECs were seeded onto PDMS samples at a density of 6000 cells/cm^2 in serum-free DMEM. For morphology and orientation studies, cells were incubated for 1, 4, 24, and 48 h. Four hours after seeding, the serum-free DMEM was removed and replaced with fresh DMEM containing 10% FBS. DMEM with 10% FBS was changed daily for longer culture times (≥24 h). To study proliferation, cell density was determined at 1, 24, 48, and 72 h using phase contrast microscopy from six random fields observed at 10× magnification.

Immunofluorescence

At the termination of each experiment, the PDMS samples were first rinsed twice in PBS to remove nonadherent cells. The attached cells were then fixed in 4% formaldehyde for 20 min at room temperature, followed by two washes with PBS. Cells were permeabilized in 0.1% Triton X-100 for 3 min, washed twice with PBS, and blocked in 1% BSA solution for 30 min. All primary and secondary antibodies were diluted in PBS. Following incubation at room temperature for 60 min with 1:200 mouse antivinculin, samples were washed with PBS three times, 10 min per washing, and then incubated for 45 min at room temperature in a solution containing 1:1000 FITC-conjugated goat antimouse and 1:1000 TRITC-conjugated phalloidin. The samples were finally washed three times, 10 min each, in PBS before mounted onto microscope glass slides. After adding a 20-μL drop of Vectashield, each sample was covered with a glass cover slip, and examined by conventional and confocal fluorescence microscopy.

Scanning electron microscopy

After rinsing the PDMS samples twice in PBS, the attached cells were fixed with 1% gluteraldehyde in 0.1 *M* sodium cacodylate buffer on ice for 40 min. The samples were then washed three times, 5 min each, with the same buffer, followed by rinsing with tissue culture water. Using 5-min immersion times, cells were dehydrated sequentially in ethanol:water mixtures containing 15, 30, 50, 70, 90, and 100% ethanol, and then twice in 100% ethanol. The dehydrated samples were critical point dried in CPD 7501 (SPI Supplies, West Chester, PA), sputter coated with gold-palladium, and examined in the SEM at an acceleration voltage of 10 keV.

Image analysis

To quantify cell orientation and morphology, the angle of cells with respect to the channel direction, cell length, and cell area were determined using Northern Eclipse software (Empix Imaging Inc, Cheektowaga, NY). The major and minor axes were defined by the long direction of the cell body and the direction perpendicular to the major axis, respectively. The angle between the major axis and the channel direction was used to categorize cell orientation. Because the smooth surfaces lacked an internal direction, cell orien-

TABLE II
Grating Dimension on Grooved PDMS Replicas

PDMS	Ridge (μm)	Channel (μm)	Depth (μm)
200 nm	3.99 (±0.76)	3.85 (±0.31)	0.19 (±0.01)
500 nm	3.46 (±0.08)	3.73 (±0.05)	0.49 (±0.02)
1 μm	3.32 (±0.25)	3.62 (±0.84)	0.98 (±0.02)
5 μm	5.51 (±0.12)	2.65 (±0.40)	4.59 (±0.03)

tation was defined relative to arbitrary axes defined as north–south (N-S) and east–west (E-W). Using cells stained with TRITC-labeled phalloidin, the ratio of cell major axis to cell minor axis was used to define an elongation index. The projected area was also measured for TRITC-labeled cells. All values were reported as mean ± standard error of mean, where $n = 250$ to 300 for orientation and $n = 50$ to 60 for elongation and area. The statistical significant of the differences ($p < 0.05$) was determined by one-way analysis of variance (ANOVA) (SigmaStat, Richmond, CA), followed by post hoc Student *t*-test.

RESULTS

Substrate characterization and fibronectin adsorption

Using AFM and SEM, the smooth and grooved substrates were inspected for quality control purposes. The vertical and lateral dimensions are tabulated in Table II. For grooved substrates with 200-nm, 500-nm and 1-μm deep channels, the widths of the ridges and channels were relatively constant, about 4 μm, with a pitch of 8 μm. For the 5-μm deep channels, the widths of the ridges and channels were 5.51 (±0.12) and 2.65 (±0.40) μm, respectively, yielding a similar pitch as the other three grooved substrates. For smooth surfaces, the average RMS roughness values were 1.4 (±1) nm over 10 μm × 10 μm scan areas analyzed by AFM. The average water contact angle on smooth surface was 109° (±4°), consistent with the hydrophobic nature of PDMS and previously reported values.[27,30]

By measuring the relative fluorescence intensity and using the method described by Toworfe et al.,[27] the average *Fn surface density was identical on all smooth and grooved PDMS substrates and estimated to be between 300 and 350 ng/cm^2 ($p \geq 0.05$). This result is consistent with a reported surface density of 350 ng/cm^2, as previously measured for I^{127}-labeled Fn adsorbed to hydrophobic bacterial and untreated polystyrene.[28] Using fluorescence microscopy (not shown), we ascertained that the intensity of *Fn was spatially uniform across all PDMS substrates. Based on these studies, the smooth and grooved substrates are homogeneously covered with a saturating density of Fn. Thus, the variations in cell morphology and orientation on the various substrates can be attributed to surface topography rather than surface chemistry.

Cell morphology

Whereas cells display a polygonal shape with random orientation on smooth substrates, endothelial cells seeded on grooved substrates exhibit an elongated shape with their long axes oriented along the channel direction. Figure 1(A–C) shows representative phase contrast images of endothelial cells on smooth, 200-nm and 1-μm substrates, respectively. On smooth PDMS [Fig. 1(A)], cells were either round or elongated in a random direction. For channel depths of 200-nm to 5-μm, a majority of cells exhibited a directional, elongated shape in response to the underlying topographic variations. On 200-nm PDMS [Fig. 1(B)], most elongated cells extended their major axes either parallel to the channels or, occasionally, across several ridges and channels. The alignment of the cells' major axes relative to the channel direction increased as the channel depth increased. For 500-nm (not shown), 1-μm [Fig. 1(C)] and 5-μm (not shown) substrates, a majority of cells aligned parallel to the direction of channels. The filopodia anchoring on the ridge edge, indicated by the white arrows in Figure 1(B) and (C), suggest that cells are able to interact not only with the channels but also extend into the channels via cell protrusions.

To further examine cell anchoring, SEM was used to visualize how cells spread on smooth as well as grooved PDMS substrates. In all cases, cells appear to spread in a conformal manner over the ridges and channels. Figure 2 shows selected top view [Fig. 2(A)] and side views [Fig. 2(B) and (C)] SEM images of cell spreading on 200-nm and 1-μm substrates, respectively. Figure 2(A) showed that filopodia (left arrow) could spread along the sidewalls of the 1-μm substrates and even extend into the channel. Moreover, filopodia extensions were found to cross the bottom of the channel (right arrow), move up the sidewall, and continue across the ride surface. These observations were consistent with the phase contrast image in Figure 1(C). Figure 2(B) and (C), side views of the 200-nm and 1-μm substrates, respectively, suggest the conformal spreading of cells on the ridges, sidewalls, and channels. Because SEM sample preparation required cell dehydration, adhesion between cell and channel floor was further studied with confocal microscopy as described later.

Cell shape: orientation, elongation, and area

Several parameters have been used to describe cell shape and cell spreading.[13,18,19,24,31] For comparison

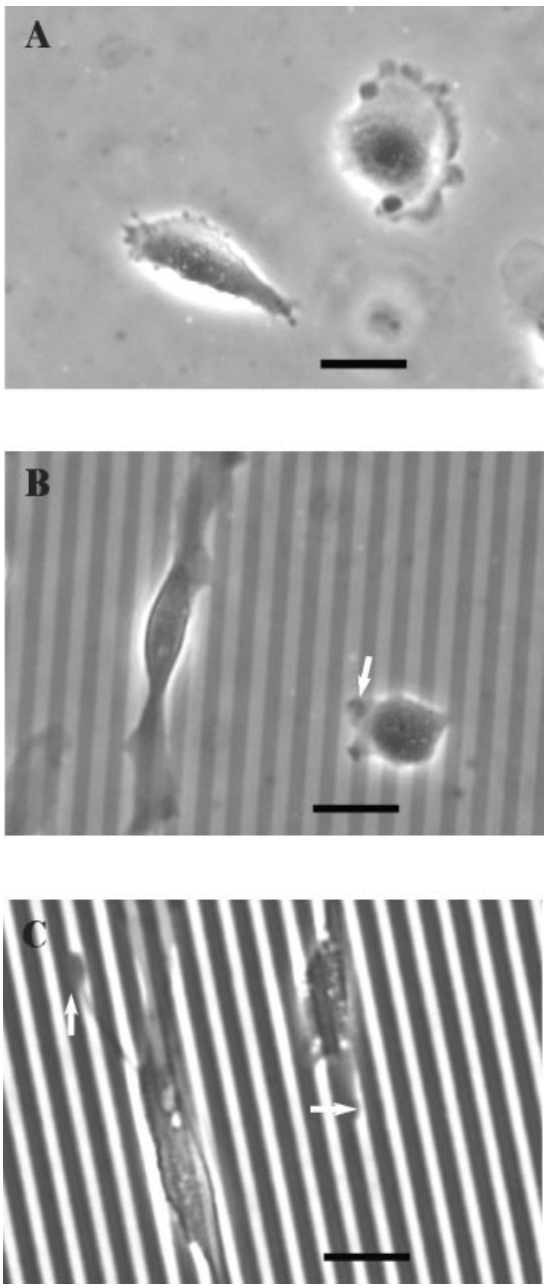

Figure 1. Phase contrast microscopy images of BAECs on smooth (A), 200-nm (B), and 1-μm (C) PDMS after incubation for 1 h. (A) Cells on smooth surfaces exhibited round (right) or randomly oriented, elongated (left) shapes. In (B) and (C), the ridges are light. (B) For 200-nm deep channels, cells elongated along the channel (left) as well as across the channel, and some remained isotropic (right). Nevertheless, lamellipodia protrusions are observed (white arrow) on the ridges suggesting that cells sense topographic variations as low as 200 nm. (C) A majority of cells elongated parallel to the channel on 1-μm PDMS. The white arrows indicate cell protrusions hugging the corners of the ridges and channels. Scale bars are 20 μm.

with previous studies, cell orientation, elongation, and projected area were used to quantify the morphological response of cells spreading on PDMS substrates inscribed with channels and grooves.

Cell orientation

Cells were described as aligned, nonaligned, or isotropic by measuring the angle between the major axes and the direction of the channels. Elongated cells were defined as aligned if their major axes were within $\pm 20^{\circ}$[18] with respect to the channel direction, and non-

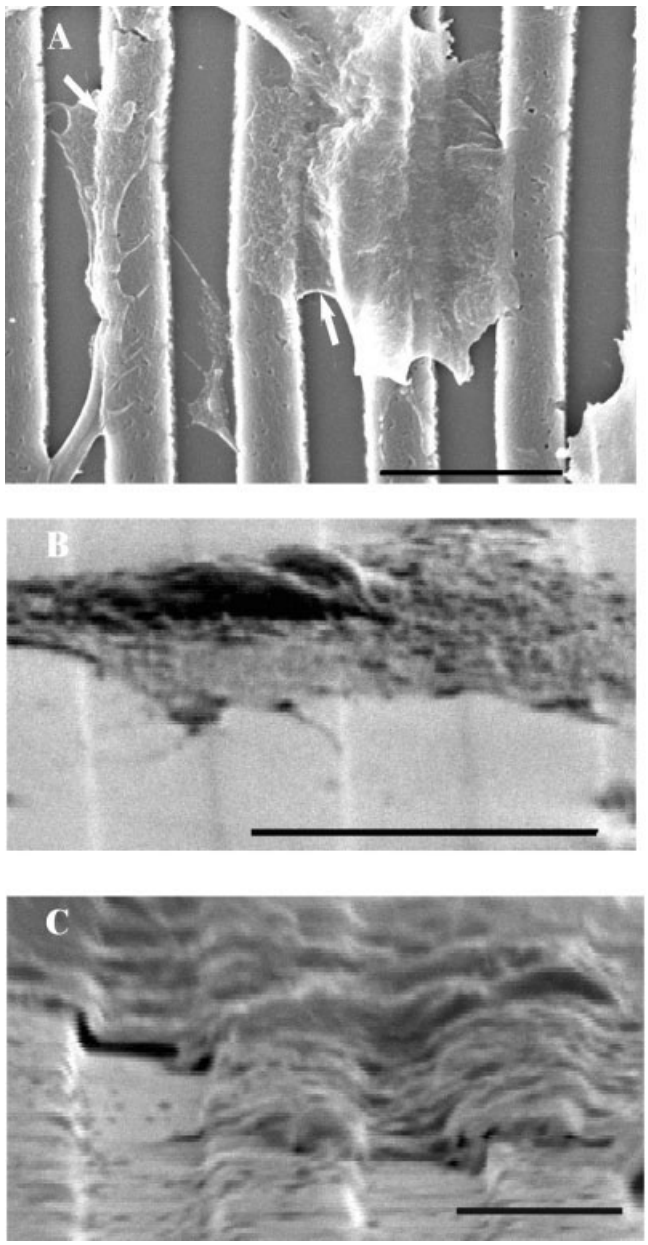

Figure 2. Scanning electron micrographs of BAEC spreading on grooved PDMS surfaces after incubation for 24 h. (A) Top view of cell spreading on 1-μm PDMS. The ridges are in light contrast. The white arrows indicate cell protrusions that span the sidewall (left) and the bottom of the channel (right). (B) and (C) side views of cells on 200-nm and 1-μm PDMS, respectively. Cells appear to follow the contour of the topography, namely along ridges, sidewalls, and the channel floor. Scale bars are 10 μm for (A) and (B) and 5 μm for (C).

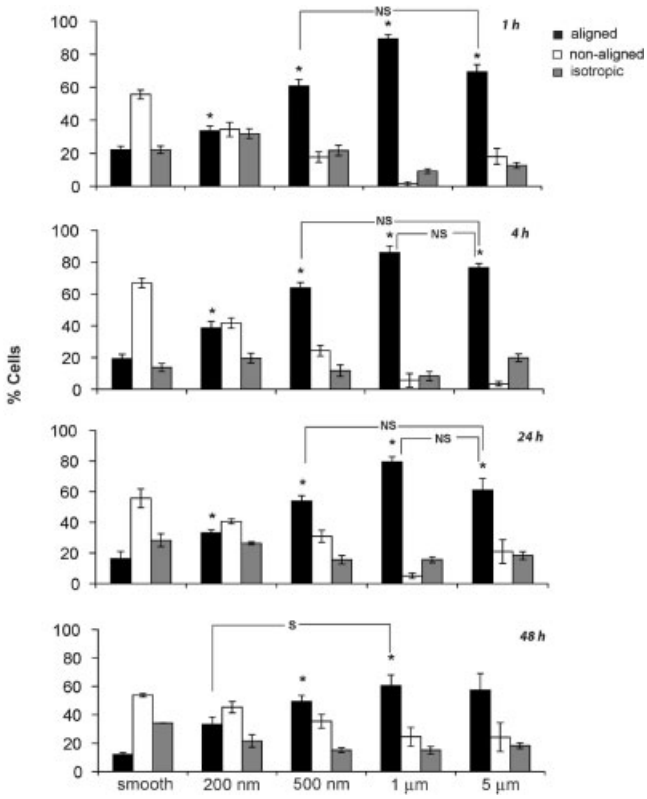

Figure 3. Percentages of endothelial cell identified as aligned (black), nonaligned (gray), and isotropic (white) on smooth and grooved PDMS surfaces at 1, 4, 24, and 48 h. As channel depths increased from 200 nm to 1 μm, cell alignment increased. The decrease in alignment for channel depths of 5 μm is attributed to the narrowing of the channel width for this particular substrate. For channel depths greater than 200 nm, a majority of the cells were aligned parallel to the channel direction for all incubation times. The asterisk (*) denotes the significant difference ($p < 0.05$) between the percentages of aligned cells on grooved surfaces and smooth surfaces. For the grooved surfaces, NS and S correspond to not significant and significant, respectively.

aligned if their major axes ranged from 20 to 90°. Isotropic cells either spread uniformly, like a disk, or exhibited randomly oriented extensions equidistant from the center of cell body.

Figure 3 shows a histogram of the percentage of aligned (black), nonaligned (gray), and isotropic (white) cells on smooth and grooved substrates after 1, 4, 24, and 48 h. Within 1 h, cell orientation was clearly established on all grooved PDMS surfaces. On smooth substrates, the percentage of "aligned" cells ranged from 10 to 20% for all four culture times, consistent with the probability (40°/180° = 22%) that a fraction of the cells will randomly orient along the N-S and E-W directions. Compared to the smooth substrates, the percentage of aligned cells on grooved surfaces was significantly higher ($p < 0.05$). Alignment increased linearly from about 30 to 90% as channel depth increased from 200 nm to 1 μm and then slightly decreased to about 60% for the 5 μm case. The maximum alignment was achieved on the 1-μm surface where 90% of the cells aligned with the channel direction. For substrates with channel depths of 500-nm, 1-μm, and 5-μm, the percentage of aligned cells was significantly greater than that of the nonaligned and isotropic cells.

As the incubation time increased to 24 h, cells remained predominantly aligned ($p < 0.05$) on 500-nm (50%), 1-μm (80%) and 5-μm (60%) surfaces despite the gradual increase (5–10%) in the percentage of nonaligned cells. Cell alignment remained strongest on the 1-μm surface for times up to 24 h. At 48 h, the trend of cell orientation with channel depth was consistent with the earlier times, although the percentage of aligned cells decreased on all grooved surfaces. A comparison of the 200-nm, 500-nm, and 1-μm surfaces having the same ridge and channel widths shows that an increase in channel depth, even by only a few hundred nanometers, can strongly enhance cell guidance to align along the channel direction.

Cell elongation

The elongation index is the second parameter used to quantify how cells respond to changes in substrate topography. Across smooth and grooved PDMS surfaces (Fig. 4), the elongation index was at all times significantly ($p < 0.05$) greater on 1-μm deep channels than on smooth, 200-nm and 500-nm surfaces. On smooth, 200- and 500-nm surfaces, the elongation indices increased from 3 to 4 at 1 h to the maximum values of 4 to 5 at 4 h; these maximum values were maintained up to 48 h. For cells on 1-μm and 5-μm substrates, however, the elongation indices reached their maximum values of 5 to 7 at 1 h and remained within this range until 48 h. Consistent with cell orientation behavior (Fig. 3), cell elongation on grooved PDMS varied with channel depth, and was strongest on 1-μm PDMS for all four culture times.

Cell area

The projected cell area on smooth and grooved PDMS substrates is plotted as a function of culture time in Figure 5. During the first 24 h, the average projected cell area on all substrates increased from 800 μm^2 to about 1200–1400 μm^2. These values of the maximum area are similar to those for BAECs in DMEM with 10% FBS on tissue culture polystyrene (control, not shown), and BAECs in a serum-containing medium on RGD-modified biodegradable polymers.[5]

Although the cell area increased between 4 h and 24 h for all substrates, it was not significantly different among the smooth and grooved surfaces at 24 h. At

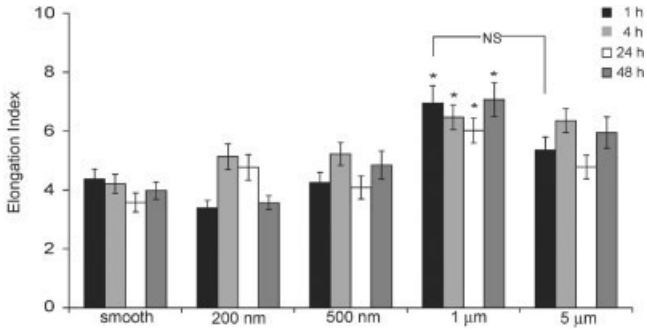

Figure 4. The elongation index of BAECs on smooth and grooved PDMS substrates for incubation times of 1, 4, 24, and 48 h. Comparing all surfaces, the elongation index was greatest ($p < 0.05$) for cells on the 1-μm PDMS for all four incubation times as indicated by the asterisk. Comparing only the grooved surfaces, NS denotes not significant and is only shown for one example at 1 h. At 4 h, differences in the elongation indices are not statistically significant for the grooved surfaces. At 24 h, there is no statistical significance in elongation indices between the 1-μm and 5-μm surfaces as well as the 1-μm and 200-nm surfaces. At 48 h, only the difference in the elongation indices for the 1-μm and 5-μm surfaces is not significant.

48 h, the cell area slightly decreased for most substrates, possibly due to the proximity of neighboring cells. A comparison of cell areas on smooth and grooved PDMS at 24 h and 48 h ($p > 0.05$) suggests that the topographic features, while not hindering cells from increasing their areas, directed the cell shape to become elongated and aligned with the channel direction as inferred from cell orientation (Fig. 3) and elongation index (Fig. 4), respectively.

Organization and alignment of F-actin and focal adhesion complex

In addition to modulating cell morphology and cell alignment, the grooved substrates also guided intracellular F-actin and focal adhesions to align parallel to the channel direction. Figure 6 shows the formation of dense peripheral F-actin bundles as well as focal adhesions after 1 h. The focal adhesions were approximately 1 μm wide and 1 to 5 μm long, consistent with literature values.[32,33] In accordance with the orientation and localization of the majority of F-actin, particularly on 500-nm, 1-μm, and 5-μm grooves [Fig. 6(C–E)], the majority of focal adhesions also aligned parallel to the channel direction and preferentially attached to the ridge edge as indicated by white arrows in Figure 6(H–J). Even for partially aligned cells, focal adhesions and F-actin (white arrows) were aligned in parallel to the channel direction as shown in Figure 6(B) for the 200-nm substrate. This preferential alignment of focal adhesions has previously been reported by Oakley and Brunette[24] and den Braber et al.[13] in their studies of fibroblasts spreading on the grooved titanium (Ti) and silicone substrates, respectively. These results in our study demonstrate that the alignment of F-actin and focal adhesions are extremely sensitive to channel depth, and can be induced by channels as shallow as 200 nm. In contrast, both F-actin and focal adhesions of cells on smooth PDMS surface were randomly oriented without any preferential alignment as shown in Figure 6(A) and (F).

Using confocal microscopy, focal adhesions on the 1-μm (Fig. 7) and 5-μm (not shown) surfaces obtained at 24 h were found to preferentially attach along the sidewalls of the channels rather than only on the ridge edge. The arrows in Figure 7 show that a majority of focal adhesions organized along the ridge edge, the channel edge and the sidewall of the channel. In a few cases, focal adhesions were found on the channel floor or the central portion of the ridge. On the 5-μm surface (not shown), focal adhesions were observed along the sidewalls as cells extended down part of the channel depth, and a majority of focal adhesions were localized on the ridge edge. In contrast to the 1-μm channel, focal adhesions were never observed on the floor of the 5-μm channel. This observation combined with the cell alignment data at 24 h (cf. Fig. 3) suggests that the different channel widths for the 1-μm and 5-μm cases do not play a significant role for this particular study.

The development of F-actin and focal adhesions depended on the culture time. After 1 h [Fig. 6(F–J)] and 4 h (not shown), vinculin was associated with focal adhesions as expected, but also distributed in the perinuclear area, suggesting the possibility of *de novo* synthesis. At 24 h (Fig. 7), mature F-actin was aligned with the cell major axis along the channel direction, whereas focal adhesions were found throughout the cell body. Assembly and alignment of both F-actin and focal adhesions remained unaltered for up to 48 h. In

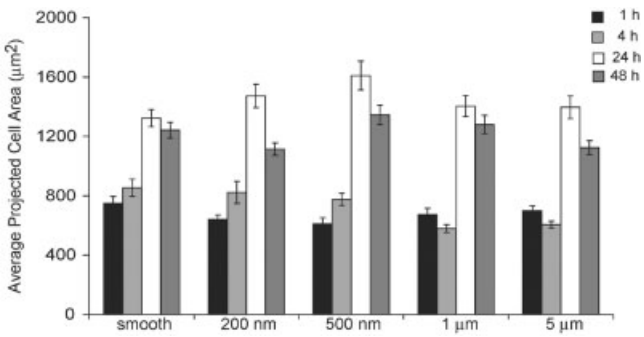

Figure 5. The average projected area of BAECs on smooth and grooved PDMS after incubation for 1, 4, 24, and 48 h. For all cases, the cell area increases between 1 h and 24 h, reaching a maximum value of 1300–1600 μm². Between 24 h and 48 h, a slight decrease in area is observed on the 200-nm, 500-nm, and 5-μm PDMS substrates.

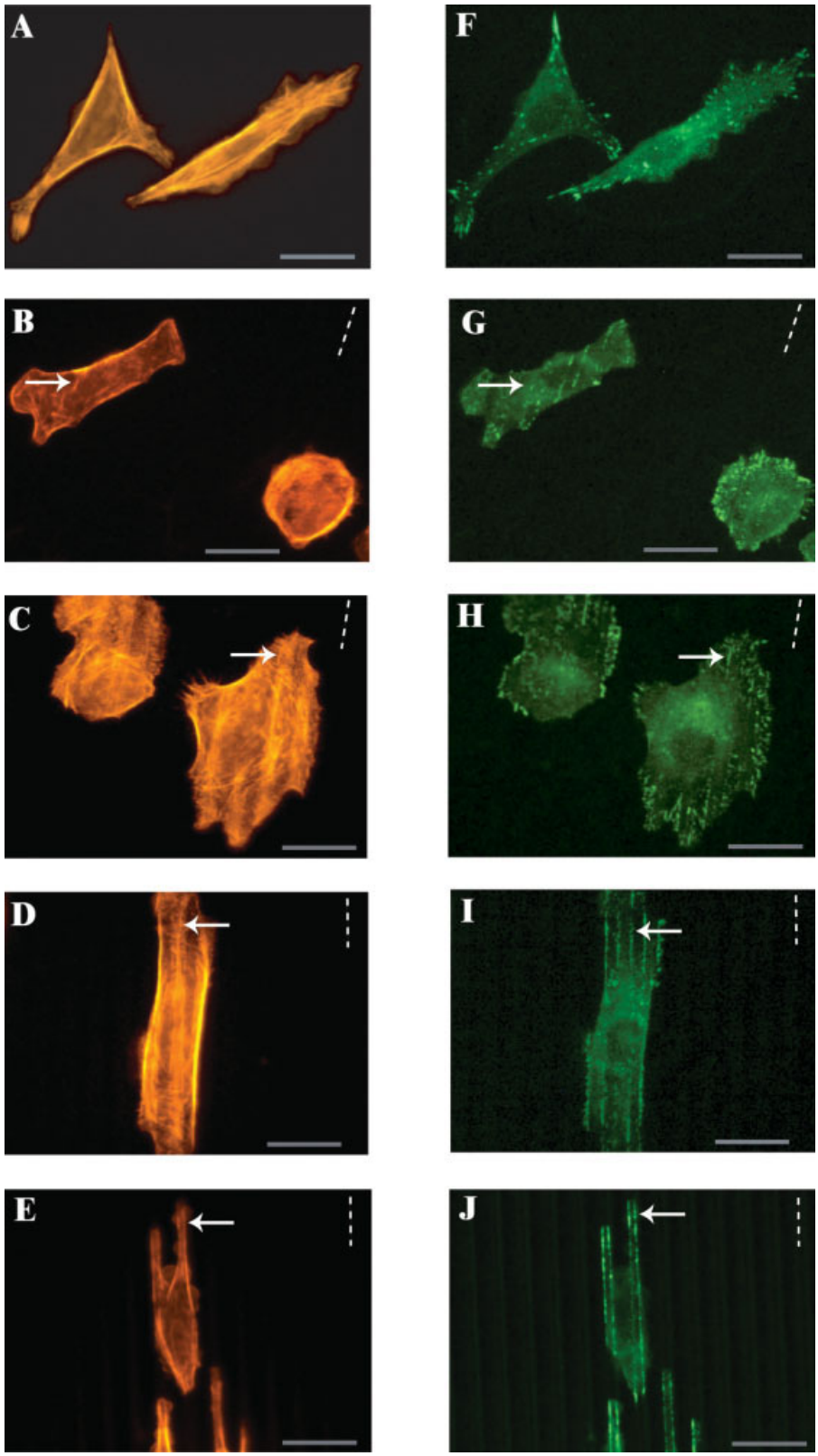

Figure 6. Organization of the cytoskeleton components, F-actin and focal adhesions, of BAECs at 1 h after incubation. Fluorescence images A–E represent F-actin staining (orange) on smooth, 200-nm, 500-nm, 1-μm, and 5-μm PDMS, and the corresponding vinculin staining (green) at focal adhesions are shown in images F–J. The direction of channels on the grooved substrates is given by the dashed lines. Solid white arrows indicate preferential alignment of F-actin and focal adhesions parallel to the channels. Scale bars are 20 μm. [Color figure can be viewed in the online issue, which is available at www.interscience.wiley.com.]

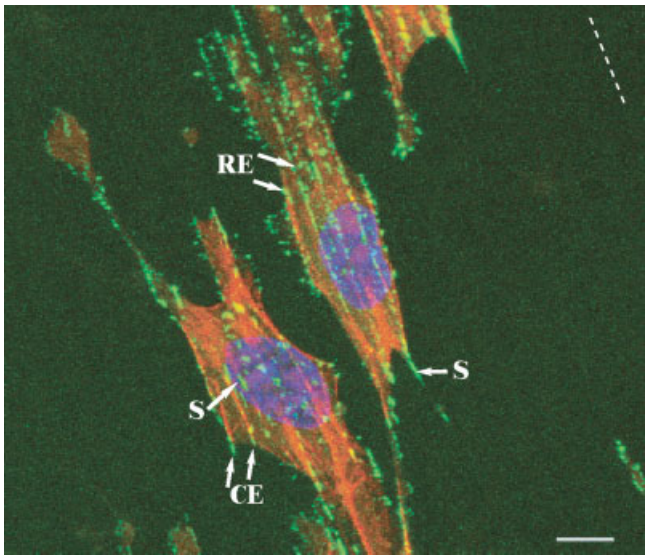

Figure 7. Overlay confocal microscopy image of cells stained for the nucleus (blue), F-actin (red), and vinculin (green) on 1-μm PDMS at 24 h incubation. This master image was reconstructed from a series of individual confocal microscopy images focused first on the channel floor and then in 0.25 μm steps along the Z-direction (i.e., up the channel) until the body of the cell could be imaged above the ridge. The white arrows show that the preferential locations of the focal adhesions are along the channel edge (CE), along the sidewalls of the channel (S), and at the ridge edge (RE). The dashed line denotes the direction of channels. Scale bar is 10 μm. [Color figure can be viewed in the online issue, which is available at www.interscience.wiley.com.]

contrast to the rapid changes in cell morphology, where maximum cell alignment were achieved after just 1 h, the maturation of the F-actin and the assembly of vinculin at focal adhesions required much longer times, about 24 h.

Cell proliferation

Figure 8 shows the increase in cell density as a function of culture time for smooth and grooved substrates. The fluorescence microscopy images show that cell populations reached near confluence at 72 h on all substrates. Cell density was similar on the smooth and grooved surfaces at 48 h and 72 h ($p > 0.05$). This unimpeded proliferation of BAECs on our grooved PDMS was consistent with studies by den Braber et al.[34] for fibroblasts on microgrooved silicon. In addition to providing cell density, the images in Figure 8 showed that the alignment of cells and F-actin was maintained at near confluence for all grooved surfaces.

DISCUSSION

The adhesion of cells to biomaterials can be mediated by the binding of cell surface integrins to ligands, typically ECM proteins, adsorbed on the substrate surface. In their resting state, arterial endothelial cells express predominantly integrins $\alpha_5\beta_1$, $\alpha_V\beta_3$, and $\alpha_2\beta_1$, which are receptors for the ECM proteins fibronectin, vitronectin, and collagen, respectively.[6] In the present study, all PDMS substrates, smooth and grooved

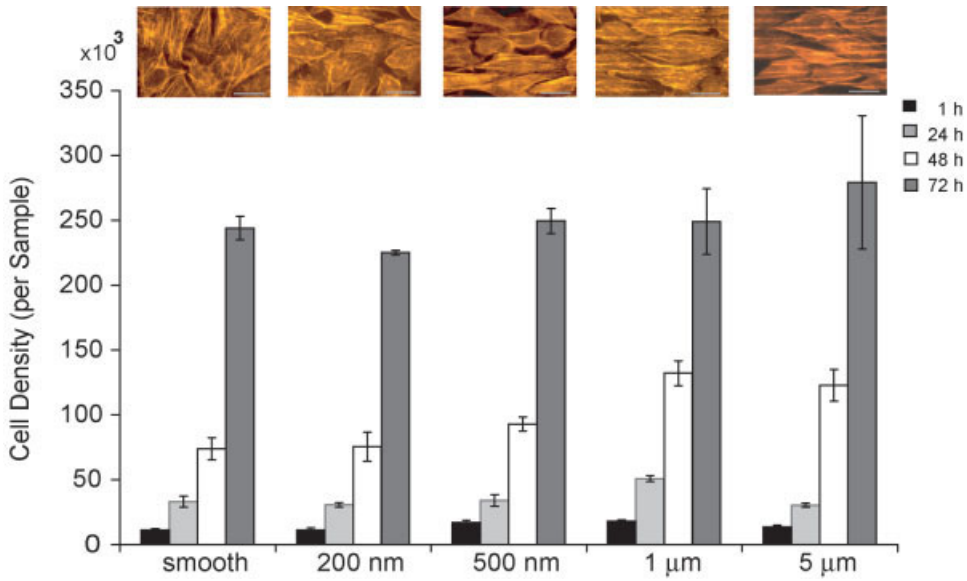

Figure 8. Cell proliferation on smooth and grooved PDMS surfaces. The fluorescence microscopy images (across top) show the orientation of F-actin (orange) for cells near confluence. The channel direction is from left to right. The scale bars are 25 μm. The cell density increased with incubation time with a maximum density at 72 h for all surfaces, corresponding to near confluence conditions. [Color figure can be viewed in the online issue, which is available at www.interscience.wiley.com.]

alike, were uniformly covered with the same areal density of fibronectin. Because of this, the ability of fibronectin to promote integrin-mediated adhesion of endothelial cells was similar for all substrates. Hence, these experiments were designed to focus on the effect of surface topography on cell shape and orientation while holding surface chemistry constant during the attachment stage.

We hypothesized that variation in channel depth on grooved PDMS can effectively induce endothelial cells to align and elongate parallel to the direction of channels similar to the shear-resistant elongated endothelium in the direction of blood flow. In line with our hypothesis, phase contrast microscopy confirmed that BAEC alignment increased as channel depth increased. In addition, conventional and confocal fluorescence microscopies showed that intracellular F-actin and focal adhesions also aligned along the channel direction. At near confluence, the alignment of cell shape and F-actin were maintained on grooved PDMS, supporting our hypothesis that the elongated endothelium can be induced by the grooved topography.

There are several unique aspects to the current study. Whereas our results show alignment of cell shape, F-actin, and focal adhesions parallel to channels in agreement with prior studies,[4,8,13,15,17–22] we further demonstrate that the alignment of BAECs persisted until near confluence on PDMS substrates with channels deeper than 500 nm. Thus, the uniformly elongated endothelium, similar to linear vessels,[9] can be structurally replicated using chemically and physically modified synthetic surfaces designed to elicit cell attachment and orientation. The preferential alignment of focal adhesions along the channel direction suggests that strong adhesion sites also form in this direction. In addition, the distribution of focal adhesions on the vertical ridge edge, along the sidewall, and on the channel edge of the 1-μm deep channels provides insight about the contribution of the cytoskeleton on cell orientation.

The progression of endothelial cell morphology and alignment depended on the dimensions of both the lateral and vertical features engraved in PDMS substrates after initial attachment. Although the widths of ridges and channels (3 to 4 μm) were smaller than the cell diameter (in suspension), a majority of cells that attached were able to spread over several ridges and channels rather than spread only on the ridge or within a channel. Using phase contrast imaging for the first 15 min after seeding, real-time video clips (not shown) showed that a round cell in suspension initially attached across two ridges and two channels, interrogated its surrounding with lamellipodia, and then spread and elongated along the surface.

By keeping the ridge width nearly constant and varying only the channel depth from 200 nm to 1 μm, grooved surfaces with a channel depth of 1 μm were found to induce a majority of cells, ~90%, to align parallel with the channel direction after only 1 h. Our results agree with the alignment of BHK cells on unmodified silicon surfaces.[18] In that study, 90 to 100% of the cells aligned parallel to channels at 24 h as both the channel depth increased above 1 μm and the channel width decreased to about 5 to 12 μm. We note that cell alignment on PDMS with 5-μm deep channels was decreased relative to the 1-μm case (Fig. 3). We attribute this behavior to the narrow channel width, ~2.6 μm, compared to on the other three grooved surfaces. This narrower channel width might have allowed cells to spread and extend across ridges and channels more readily than on the other substrates with a broader width but shallower channel depth. Clearly, systematic studies involving the variation of channel width at constant depth would provide important insight and understanding.

As cells spread on grooved surfaces, changes in cell morphology were accompanied by changes in the distribution of cytoskeletal components. In particular, both F-actin and focal adhesions were established and directed along the channel direction within 1 h and matured within 24 h. The alignment of F-actin in endothelial cells on grooved PDMS was previously reported. Whitesides et al.[8] observed the generation and alignment of dense actin stress fibers in bovine capillary endothelial cells on PDMS having an undulating surface with a periodicity of 5 μm. We also observed that the maturation of vinculin assembly into dense streaks at focal adhesions takes 24 h. Our result is consistent with the data of van Kooten and von Recum,[4] who observed vinculin assembly in human umbilical vein endothelial cells after 24 h for cells on silicone with a channel depth of 0.5 μm and channel spacing of 2, 5, and 10 μm. Our observation that F-actin and vinculin assembled into focal adhesions already at 1 h is in agreement with the work of Oakley and Brunette,[24] who observed the alignment of these two cytoskeletal proteins after only 40 min in human gingival fibroblasts spreading on grooved Ti with a depth of 3 μm and floor width of 11 μm. In contrast to our grooved surfaces with nearly vertical channel walls, the sidewalls and floor of the Ti groove met at an angle of 125°. Nevertheless, the distinct localization of vinculin aggregates was observed at the corner of the Ti ridge consistent with our observation that the alignment of vinculin occurred at the corners of our PDMS ridge. An interesting observation in the studies of Oakley and Brunette[24] is that their groove floor width was able to accommodate focal contacts oriented both parallel and perpendicular to the groove direction. Oakley and Brunette[24] also observed that microtubules formed and aligned within 20 min, thus preceding the alignment of F-actin and cell shape.

Thus, this study[24] suggests that the assembly and alignment of microtubules may determine early cell alignment immediately after the cells attach onto the substrate. Future studies are needed to investigate whether the rearrangement of F-actin alone can affect endothelial cell alignment in the absence of functional microtubules.

Although many studies of cell alignment[4,13,15–21] and cytoskeletal orientation[4,13,14,24] have been published, the mechanism by which cultured cells sense and respond to the underlying substrate topography is an evolving subject. Different tentative mechanisms[13] for this contact guidance have been discussed, such as (1) the effect of mechanical restriction imposed by the substrate geometry on the formation of linear bundles of F-actin,[14] (2) the limitation in ridge width that drives cells to align in the groove direction to maximize the focal contact areas,[15] and (3) the favorable distribution and conformation of adsorbed proteins on different areas of the substrate to promote preferential integrin-mediated adhesion.[13] The grooved substrates investigated in our study were designed to have a similar coverage of Fn, 300–350 ng/cm^2, and individual substrates were shown to have a homogeneous Fn distribution across the ridge, sidewall, and channel floor. In addition, the ridge width was chosen to allow vinculin assembly at focal adhesions to occur perpendicular to the channel direction. Combining these constraints in composition and geometry with the experimental observations of cell alignment and cytoskeletal alignment (cf. Figs. 6 and 7), suggests that the "mechanical restriction" hypothesis appears to best explain our data. Although microtubules, F-actin, and intermediate filaments form an interwoven network[35] that supports cell shape and movement, F-actin is the single most dominate cytoskeletal element for determining cell stiffness.[36] Thus, the effect of the topography of the substratum on cell alignment may be dominated by the behavior of the actin cytoskeleton.

The structural plasticity of cells and the stiffness of F-actin play an important role in determining whether a cell can adapt to the contours of the substrate. During the attachment of cells, dynamic "tread milling"[37] of F-actin provides cells with the flexibility to conform to changes in topography. Evidence for this flexibility is found in Figure 2, which shows that cell protrusions conform to ridges, sidewalls, and channels for grooved surfaces with 200-nm and 1-μm deep channels. The spreading of cells down the sidewalls is consistent with the observation of cells spreading down microneedle posts coated with adhesive proteins.[38] The ability of cells to adapt to groove pattern is also confirmed by the distribution of focal adhesions along the cell height (Fig. 7). Once focal adhesion is established by the clustering of ligand-bound integrins, the reorganization of F-actin into bundles and networks stiffens the cell and maintains cell shape while spreading on the substrate. Using a micropipette technique, elongated BAECs with aligned F-actin were shown to have a stiffness that was fivefold greater than round BAECs.[39]

Because cell flexibility depends, in part, on the stiffness of F-actin, a brief discussion of these F-actin and F-actin bundles may provide insight into the mechanism underlying contact guidance. The resistance to bending of these fibers results from the bending modulus of these rigid-rod biopolymers. This bending modulus is determined by the persistence length, which is the distance along the biopolymer backbone associated with a loss of spatial correlation.[40] The persistence length of a single actin filament is 10–20 μm,[40] and is expected to increase as filaments crosslink with one another to form bundles. As the bending modulus proportionally scales with the persistence length, cells can minimize the deformation energy costs by aligning F-actin parallel to the channel direction. In addition, the preferential localization of focal adhesions parallel to the channels may help support the aligned F-actin, and also serve as a termination point for F-actin that span ridges and channels. Thus, the inherent stiffness of the cytoskeletal microfilaments might significantly contribute to cell alignment in response to the underlying topography. Future experiments will investigate the effect of channel width at constant depth to determine if the reaction of cells and their cytoskeletal components can be further fine-tuned by topography.

CONCLUSION

In our study, the shape and orientation of bovine aortic endothelial cells was investigated on smooth and grooved PDMS substrates having channels and ridges with fixed widths, ~3.5 μm. At constant Fn coverage, cell alignment was strongest for substrates with 1-μm deep channels at all culture times, namely 1, 4, 24, and 48 h. Cells on the deepest channel studied, 5 μm, showed a loss of alignment, possibly because the channel width was narrower than other substrates. The alignment of cells was correlated with the formation of cytoskeletal components, F-actin and focal adhesions, which also aligned parallel to the channel direction. Cell density studies for up to 72 h suggest that the underlying topography does not strongly influence cell proliferation. Moreover, cell and F-actin alignment was maintained until confluence. Confocal microscopy

studies also showed that aligned focal adhesions formed at the corner of the ridge, along the sidewalls of the channel, and at the corner where the channel floor and sidewall meet. The location of focal adhesions at regions of high cell stress provides a mechanistic explanation for the sensitivity of cell alignment to surface topography. In response to the underlying surface topography, these studies suggest that cell orientation is mediated by the stiffness of the actin cytoskeleton.

The authors acknowledge Mr. Vladimir Dominko for his assistance with photolithography and RIE at the University of Pennsylvania's Microfabrication facility, Dr. Stephane Evoy for access to RIE, and the Penn Regional Nanotechnology Facility.

References

1. Lin H, Sun W, Mosher D, Garcia-Echeverria C, Schaufelberger K, Lelkes P, Cooper S. Synthesis, surface, and cell-adhesion properties of polyurethanes containing covalently grafted RGD-peptides. J Biomed Mater Res 1994;28: 329–342.
2. Chen CS, Mrksich M, Huang S, Whitesides GM, Ingber DE. Geometric control of cell life and death. Science 1997;276:1425–1428.
3. Mathur AB, Chan BP, Truskey GA, Reichert WM. High-affinity augmentation of endothelial cell attachment: Long-term effects on focal contact and actin filament formation. J Biomed Mater Res 2003;66A:729–737.
4. van Kooten TG, von Recum AF. Cell adhesion to textured silicone surfaces: The influence of time of adhesion and texture on focal contact and fibronectin fibril formation. Tissue Eng 1999;5:223–240.
5. Cook AD, Hrkach JS, Gao NN, Johnson IM, Pajvani UB, Cannizzaro SM, Langer R. Characterization and development of RGD-peptide-modified poly(lactic acid-co-lysine) as an interactive, resorbable biomaterial. J Biomed Mater Res 1997;35: 513–523.
6. Murugesan G, Ruegsegger MA, Kligman F, Marchant RE, Kottke-Marchant K. Integrin-dependent interaction of human vascular endothelial cells on biomimetic peptide surfactant polymers. Cell Commun Adhes 2002;9:59–73.
7. Sidouni FZ, Nurdin N, Chabrecek P, Lohmann D, Vogt J, Xanthopoulos N, Mathieu HJ, Francois P, Vaudaux P, Descouts P. Surface properties of a specially modified high-grade medical polyurethane. Surface Sci 2001;491:355–369.
8. Jiang X, Takayama S, Qian X, Ostuni E, Wu H, Bowden N, LeDuc P, Ingber D, Whitesides GM. Controlling mammalian cell spreading and cytoskeletal arrangement with conveniently fabricated continuous wavy features on poly(dimethylsiloxane). Langmuir 2002;18:3273–3280.
9. Nerem RM, Levesque M, Cornhill J. Vascular endothelial morphology as an indicator of the pattern of blood-flow. J Biomech Eng 1981;103:172–176.
10. Weiss P. In vitro experiments on the factors determining the course of the outgrowing nerve fiber. J Exp Zool 1934;68:393–448.
11. Weiss P. Nerve pattern: The mechanics of nerve growth. Growth 1941;5:163–203.
12. Weiss P. Experiments on cell and axon orientation in vitro: The role of colloidal exudates in tissue organization. J Exp Zool 1945;68:353–448.
13. den Braber ET, de Ruijter JE, Ginsel LA, von Recum AF, Jansen JA. Orientation of ECM protein deposition, fibroblast cytoskeleton, and attachment complex components on silicone microgrooved surfaces. J Biomed Mater Res 1998;40: 291–300.
14. Dunn GA, Heath JP. A new hypothesis of contact guidance in tissue cells. Exp Cell Res 1976;101:1–14.
15. Ohara P, Buck R. Contact guidance in vitro: A light, transmission, and scanning electron microscopic study. Exp Cell Res 1979;121:235–249.
16. den Braber ET, de Ruijter JE, Ginsel LA, von Recum AE, Jansen JA. Quantitative analysis of fibroblast morphology on microgrooved surfaces with various groove and ridge dimensions. Biomaterials 1996;17:2037–2044.
17. Teixeira AI, Abrams GA, Murphy CJ, Nealey PF. Cell behavior on lithographically defined nanostructured substrates. J Vac Sci Technol B 2003;21:683–687.
18. Britland S, Morgan H, Wojciak-Stothard B, Riehle M, Curtis A, Wilkinson C. Synergistic and hierarchical adhesive and topographic guidance of BHK cells. Exp Cell Res 1996;228: 313–325.
19. Clark P, Connolly P, Curtis ASG, Dow JAT, Wilkinson CDW. Topographical control of cell behavior: II. Multiple grooved substrata. Development 1990;108:635–644.
20. Meyle J, Gueltig K, Nisch W. Variation in contact guidance by human cells on a microstructured surface. J Biomed Mater Res 1995;29:81–88.
21. Wójciak-Stothard B, Curtis A, Monaghan W, Macdonald K, Wilkinson C. Guidance and activation of murine macrophages by nanometric scale topography. Exp Cell Res 1996;223:426–435.
22. Tan J, Saltzman WM. Topographical control of human neutrophil motility on micropatterned materials with various surface chemistry. Biomaterials 2002;23:3215–3225.
23. Singhvi R, Stephanopoulos G, Wang DIC. Review: Effects of substratum morphology on cell physiology. Biotech Bioeng 1994;43:764–771.
24. Oakley C, Brunette DM. The sequence of alignment of microtubules, focal contacts and actin filaments in fibroblasts spreading on smooth and grooved titanium substrata. J Cell Sci 1993;106:343–354.
25. Chesmel KD, Clark CC, Brighton CT, Black J. Culture response to chemical and morphological aspects of biomaterial surfaces. II. The biosynthetic and migratory response of bone cell populations. J Biomed Mater Res 1995;29:1101–1110.
26. Hong HL, Brunette DM. Effect of cell shape on proteinase secretion by epithelial cells. J Cell Sci 2004;87:259–267.
27. Toworfe GK, Composto RJ, Adams CS, Shapiro IM, Ducheyne P. Fibronectin adsorption on surface-activated polydimethylsiloxane and its effect on cellular function. J Biomed Mater Res 2004;71A:449–461.
28. García AJ, Vega MD, Boettiger D. Modulation of cell proliferation and differentiation through substrate-dependent changes in fibronectin conformation. Mol Biol Cell 1999;10: 785–798.
29. Manolopoulos VG, Samet MM, Lelkes PI. Regulation of the adenylyl cyclase signaling system in various types of cultured endothelial cells. J Cell Biochem 1995;57:590–598.
30. Wilson DJ, Pond RC, Williams RL. Wettability of chemically modified polymers: Experimental and theory. Interface Sci 2000;8:389–399.
31. Nerem RM. Shear force and its effect on cell structure and function. ASGSB Bull 1991;4:87–94.

32. Izzard CS, Lochner LA. Cell-to-substrate contacts in living fibroblasts: An interference reflexion study with an evaluation of the technique. J Cell Sci 1976;21:129–159.
33. Mathur AB, Truskey GA, Reichert WM. Synergistic effect of high-affinity binding and flow preconditioning on endothelial cell adhesion. J Biomed Mater Res 2003;64A:155–163.
34. den Braber ET, de Ruijter JE, Smits HTJ, Ginsel LA, von Recum AF, Jansen JA. Quantitative analysis of cell proliferation and orientation on substrata with uniform parallel surface microgrooves. Biomaterials 1996;17:1093–1099.
35. Heuser JE, Kirschner MW. Filament organization revealed in platinum replicas of freeze-dried cytoskeletons. J Cell Biol 1980;86:212–234.
36. Wang N, Butler JP, Ingber DE. Mechanotransduction across the cell surface and through the cytoskeleton. Science 1993;260: 1124–1127.
37. Alberts B, Johnson A, Lewis J, Raff M, Roberts K, Walter P. Molecular biology of the cell. New York: Garland Science; 2002.
38. Tan J, Tien J, Pirone D, Gray D, Bhadriraju K, Chen C. Cells lying on a bed of microneedles: An approach to isolate mechanical force. Proc Natl Acad Sci USA 2003;100:1484–1489.
39. Sato M, Levesque MJ, Nerem RM. Micropipette aspiration of cultured bovine aortic endothelial cells exposed to shear stress. Arteriosclerosis 1987;7:276–286.
40. Boal, D. Mechanics of the cell. Cambridge: Cambridge University Press; 2002.